Development of POS446M & POS430 Ti Flatron Rail Manufacturing Process for Practical Use

Hyun Tae Chun[b], Nam Je Koh[b*], Soo Deok Han[b*], No Jin Park[a*], and Myung Hoon Oh[a*]

Abstract

POS446M and POS430Ti alloys were investigated for application to a Flatron rail instead of conventional 28 wt%Cr alloy in order to reduce material costs. It was found that the permeability decrement of materials could be successfully minimized by proper heat treatment, and that the beam landing drift of the Flatron was not overly affected by the permeability of materials. In addition, the Flatron manufacturing process using POS430Ti was also stabilized without glass cracking by the application of the modified process conditions, which were optimized through the design of the experiment method.

Keywords : Flatron rail, POS 446M, POS430Ti, landing drift, glass crack.

1. Introduction

The size of the monitor market has been steadily increasing at more than a 10 % CAGR (Compound Average Growth Rate) since 1999 and this trend is predicted to continue through 2005. Although mostly CDT monitors have been produced thus far, it is forecasted that the TFT LCD monitor will exceed the number of CDT by 2004 in terms of sales volume because efforts have been put to desperately lower the manufacturing costs of the LCD since 1998. Therefore, in order to maintain a strong position in the market, price will be a key issue for manufacturers [1-3].

Fig. 1 shows the schematics of a Flatron and a conventional CDT. Flatron, which has a perfectly flat panel, is distinguished in PMA (Panel Mask Assembly) parts from a conventional CDT. In the present study, in order to reduce the cost of materials used in the Flatron rail, which supports the mask and has exactly the same function as the frame of a conventional CDT, we analyzed characteristics required for the Flatron rail and investigated candidate materials for a low-cost manufacturing process.

As shown in Fig. 2, a strip of raw material was deformed to an A-shaped rail by roll forming. It was then heat treated at 600℃ to relieve the residual stress incurred by the roll forming process. This rail was directly bonded to the panel using frit glass at around 450℃. After the bonding, the surface of the rail was accurately grinded to meet the required value of mask-to-screen spacing (Q-value), and the mask was then welded onto the rail with flat tension. Finally, this panel and funnel were sealed with frit and the production process was completed by evacuating of the sealed tube.

Good mechanical properties such as yield strength, elongation and hardness are required for the improvement of the fabrication process, while magnetic properties such as high permeability and low coercive force are required for a high-quality product.

Manuscript received November 19, 2001; accepted for publication March 27, 2002.
* Member, KIDS.
Corresponding Author : Myung Hoon Oh.
a. Deepartment of Materials Science & Engineering. Kumoh National University of Technology, #188, Sinpyoung-dong, Gumi-city, Gyoungbuk 730-701, Korea.
b. Device Research Laboratory, LG. Philips Displays, #184, Gongdan 1-dong, Gumi-city, Gyoungbuk 730-030, Korea.
E-mail : ohmyung@kumoh.ac.kr **Tel** : +54 467-4336 **Fax** : +54 467-4478

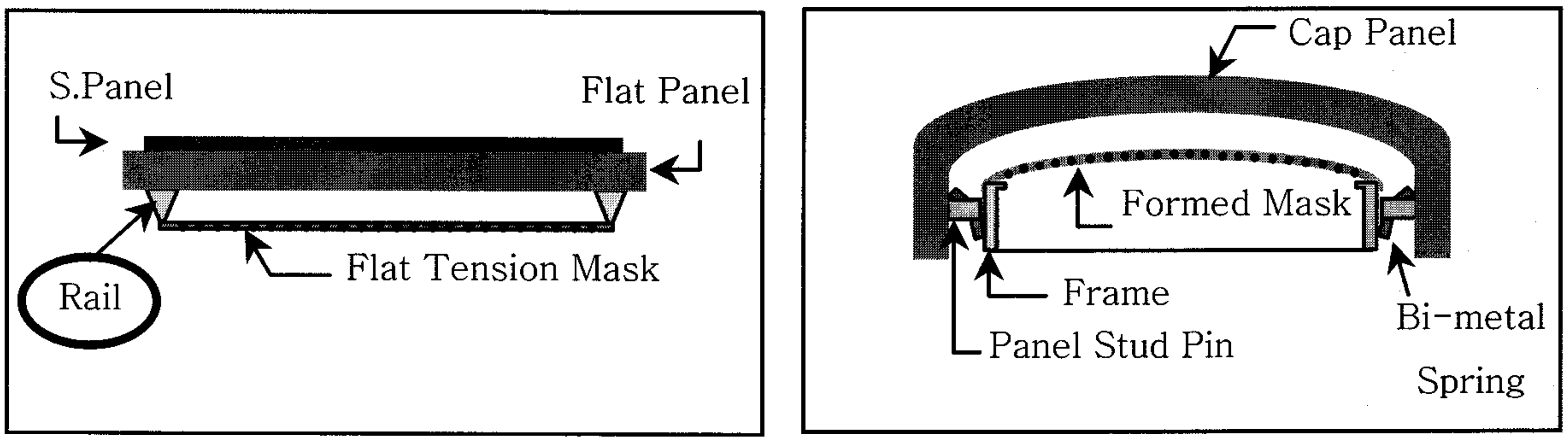

(a) Flatron PMAStructure (b) Conventional PMA structure

Fig. 1. Schematics of conventional and Flatron PMA structure for comparison.

Table 1. Nominal chemical composition of materials used in this study (wt%).

Specimens	C	Ni	Ti	Mo	Cr	Fe
POS430Ti	0.017	0.35	0.50		19	Bal.
POS446M	0.006	0.25		2.0	26	Bal.
28 %Cr alloy	0.050	0.05			28	Bal.

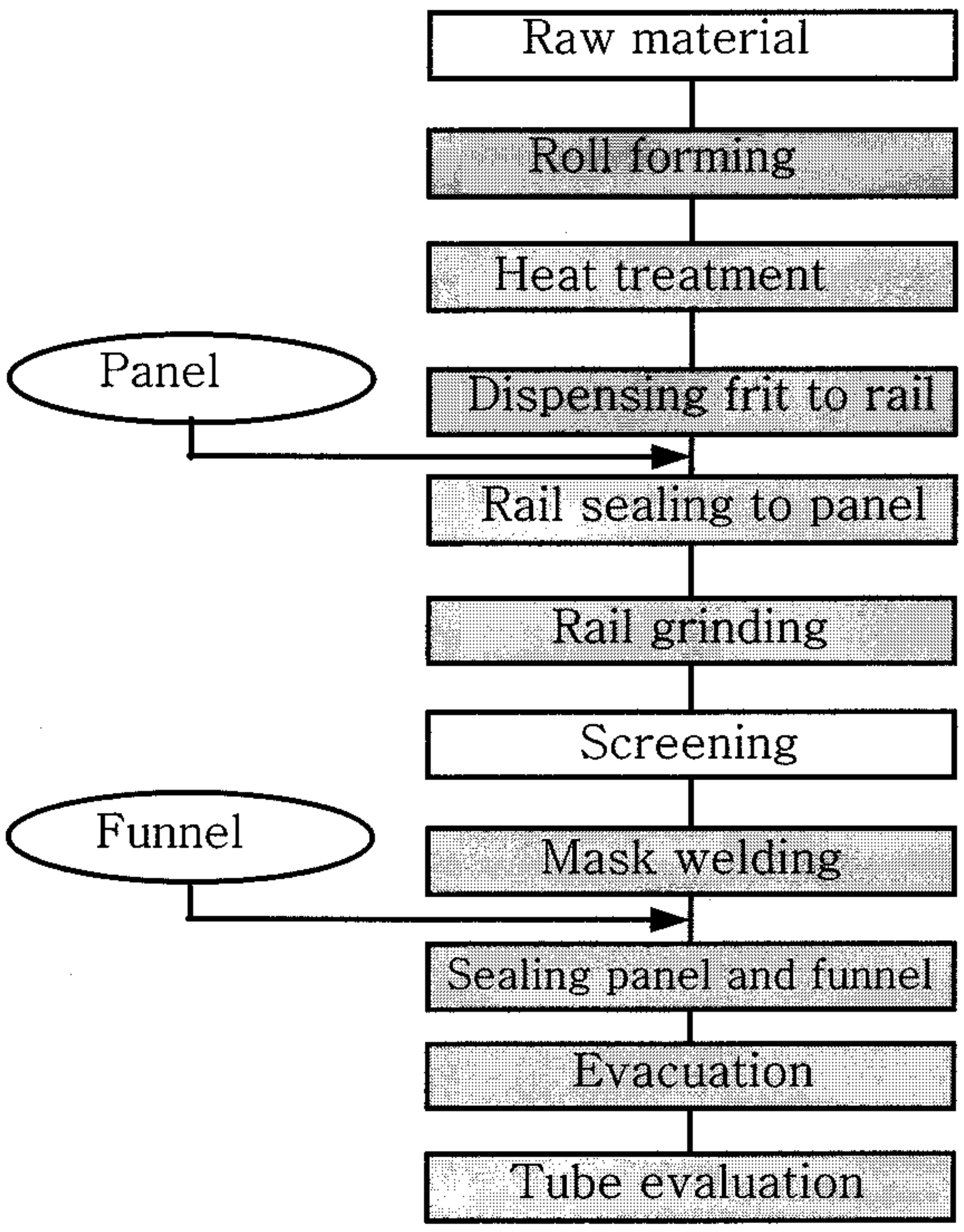

Fig. 2. Flow chart of Flatron manufacturing process concentrating on rail.

Consequently, we selected materials that would meet the above characteristics and found that POS430Ti and POS446M, procured from POSCO, were suitable. POS430Ti was developed for the stud pin of a conventional CRT and POS446M as a structural material [4-5]. These materials are similar to Fe-28 wt% Cr alloy

Table 2. Physical characteristics of materials used in this study.

Specimens	Magnetic Property		The Expansion Coefficient		Remark
	Permeability	Coercive Force	CTE	Range	
POS430Ti	513	5.0	11.5E-6	30-400℃	Glass : 10.5E-6
POS446M	532	2.9	11.0E-6	30-300℃	
28 %Cr alloy	2168	2.2	10.8E-6	30-400℃	

Table 3. Orthogonal array table of L8 (2^7) for Signal to Noise (S/N) ratio.

No	F.T	F.S	3	4	M.T	End-cap	7
1	450	Cutting	1	1	0.78	28Cr	1
2	450	Cutting	1	2	0.61	19Cr	2
3	450	Round	2	1	0.78	19Cr	2
4	450	Round	2	2	0.61	28Cr	1
5	430	Cutting	2	1	0.61	28Cr	1
6	430	Cutting	2	2	0.78	19Cr	2
7	430	Round	1	1	0.61	19Cr	2
8	430	Round	1	2	0.78	28Cr	1

Table 4. Analysis of variance for crack formation using adjusted SS for tests.

Source	DF	Seq SS	Adj SS	Adj MS	F	P
F.T	1	9.299	9.299	9.299	1.84	0.178
F.S	1	14.111	14.111	14.111	2.79	0.098
M.T	1	82.080	82.080	82.080	16.21	0.000
End-cap	1	10.408	10.408	10.408	2.06	0.154

in mechanical properties but differ from it in physical properties, as shown in Table 1. In the present work, we have studied these materials to be applied to the Flatron rail instead of conventional Fe-28 wt% Cr alloy.

2. Experimental

2.1 Preparation of raw materials

Table 1 shows the nominal chemical composition of materials used in this work. POS430Ti contains 19 wt% Cr and 0.50 wt% Ti, which prevents the precipitation of σ phase and promotes a stable oxide film of Cr_2O_3 to seal with glass [4-5]. POS446M is mainly composed of 26 wt%Cr and 2 wt%Mo to enhance anticorrosion characteristics. The 28 wt% Cr alloy has been used as a conventional rail material. For experiments, the specimens were prepared in strips of 0.61 mm in thickness and 21 mm in width. In the case of POS430Ti, another series of strips having different thickness (0.78 mm) were also prepared to examine the effects of thickness during thermal process. The physical

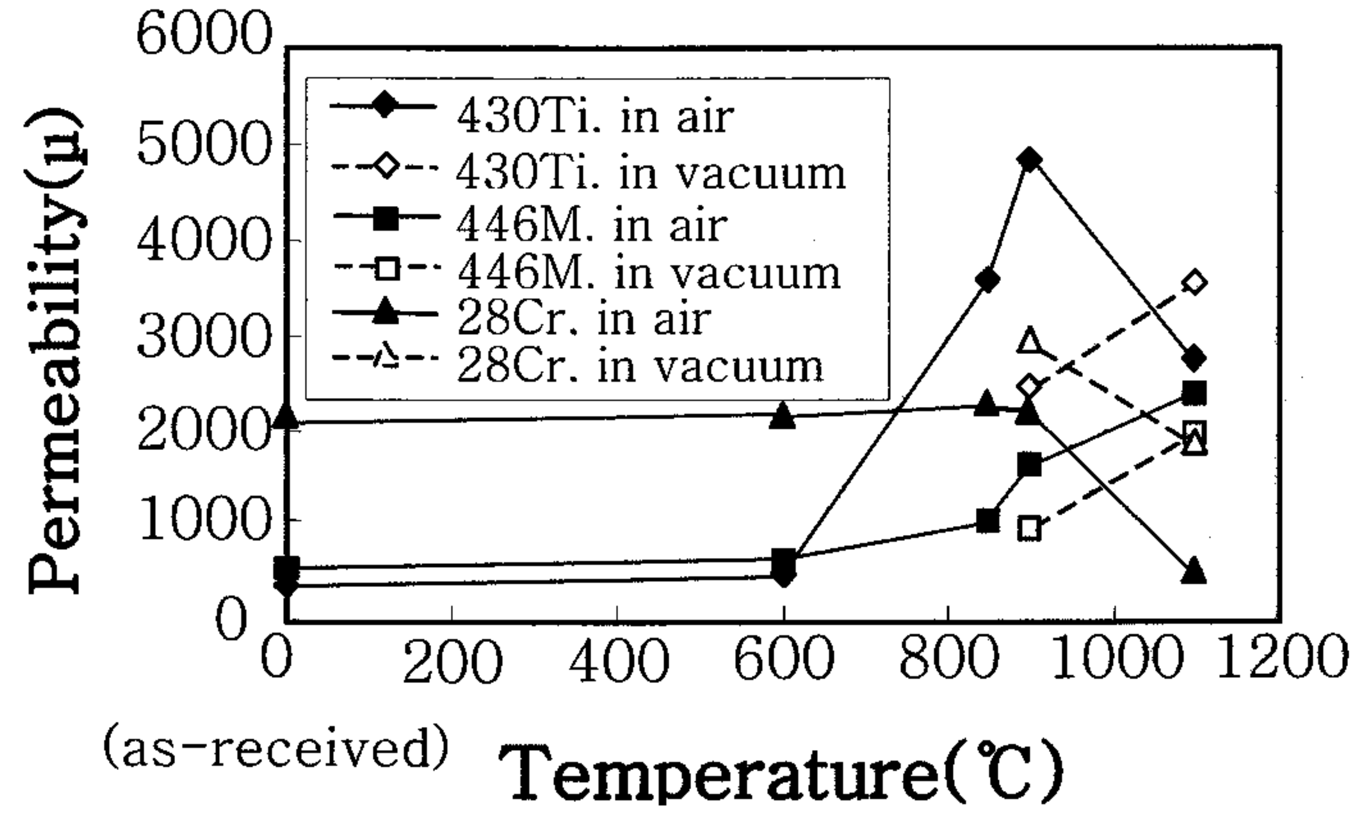

Fig. 3. Change in permeability values in accordance with heat treatment conditions.

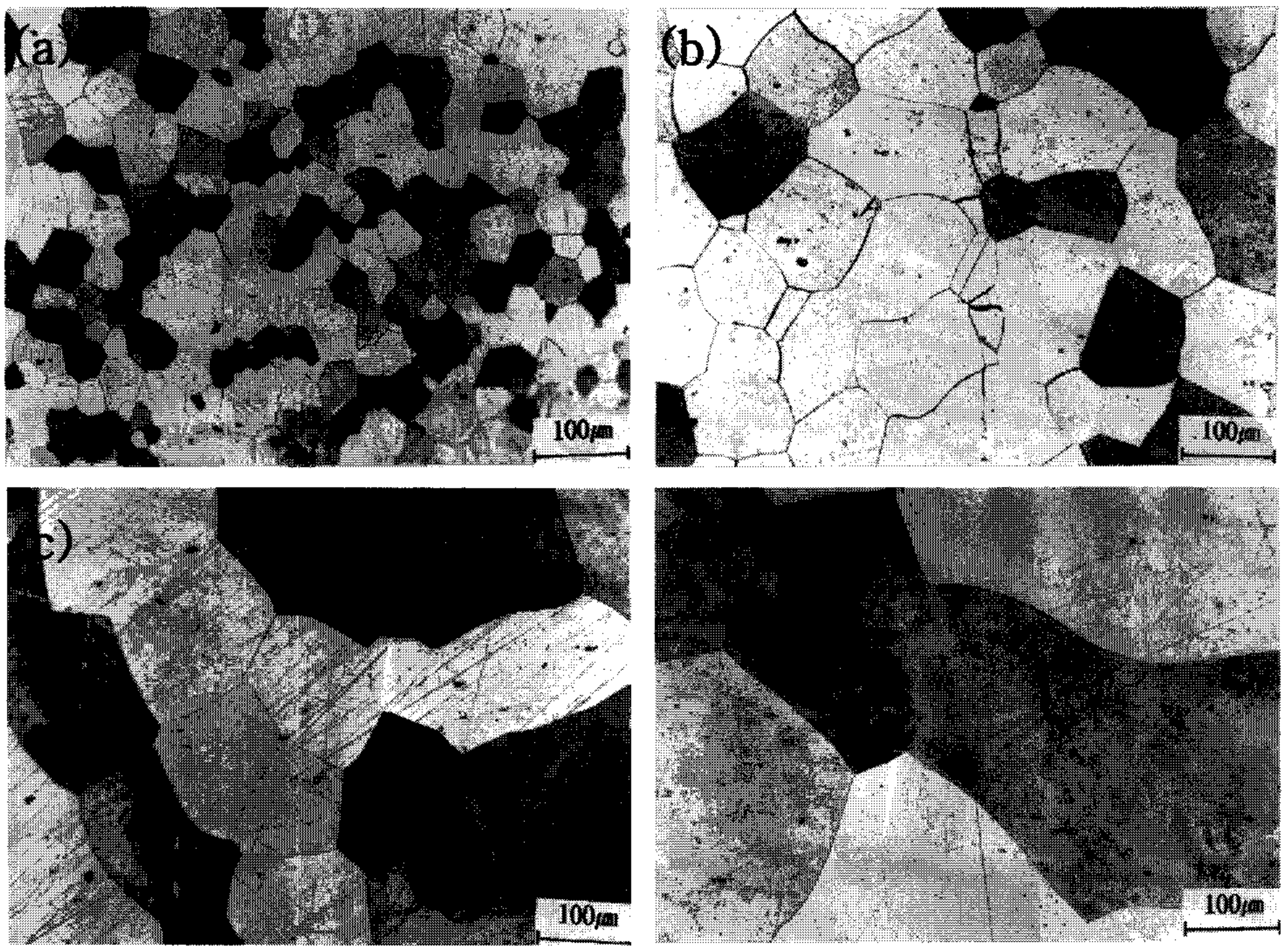

Fig. 4. Optical micrographs of POS446M, which show the change of grain size in accordance with heat treatment temperatures: (a) as-received and heat treated at (b) 600 ℃, (c) 900 ℃ and (d) 1100 ℃, respectively.

properties of the materials are presented in Table 2. The values of permeability of POS430Ti and POS446M are 24 % and 25 %, respectively, compared with the 28 wt%Cr alloy. Consequently, it is anticipated that mislanding of the electron beam for these new materials could be affected by the terrestrial magnetic field due to the difference in permeability. While the coefficient of thermal expansion of 28 wt% Cr alloy is 2.9 % higher than that of glass, POS430Ti and POS446M are 9.5 % and 4.8 % higher, respectively. Therefore, it could be expected that POS430Ti may cause cracking on the glass panel under the present thermal process conditions of Flatron fabrication.

2.2 Observation of magnetic properties depending on heat treatment temperature

Magnetic properties were measured with a LDJ5500 Hysteresigraph (magnetic measurement system) after these materials were heat-treated under an atmosphere of

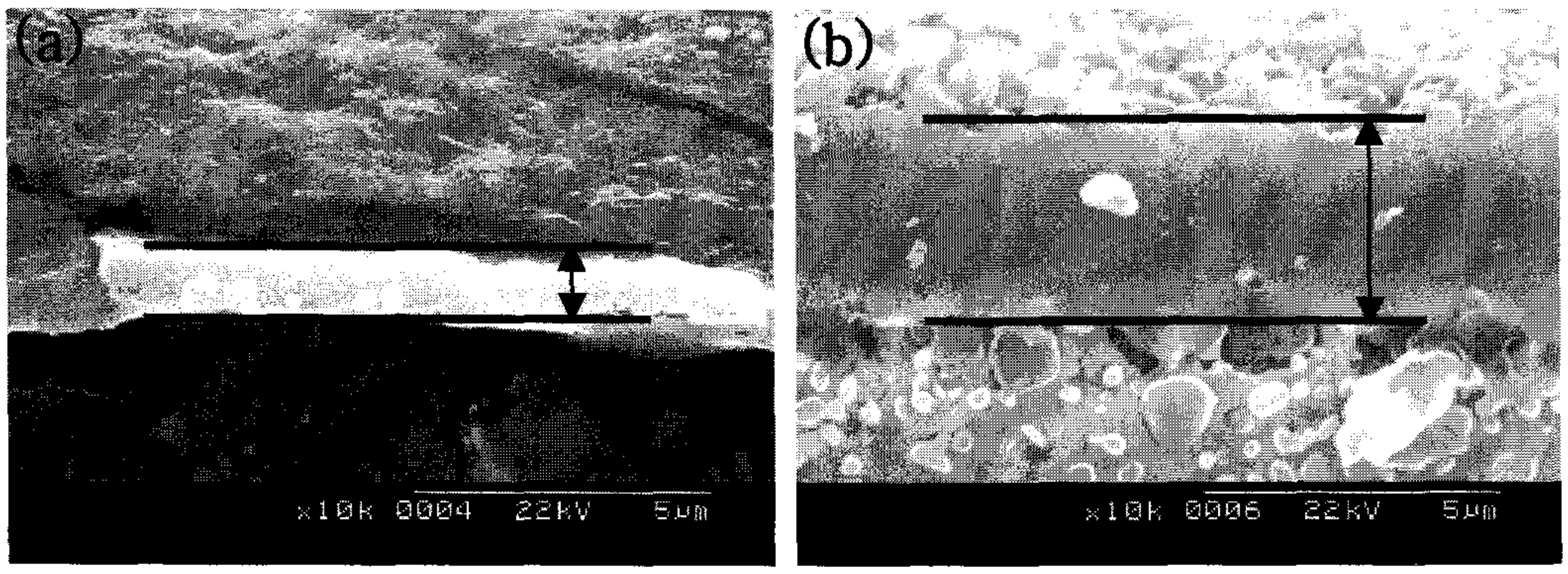

Fig. 5. SEM micrographs of POS430Ti, which show the thickness of the oxidation layer: heat treated in air at (a) 900 ℃(1.0μ) and (b) 1100 ℃(3.6 μ), respectively.

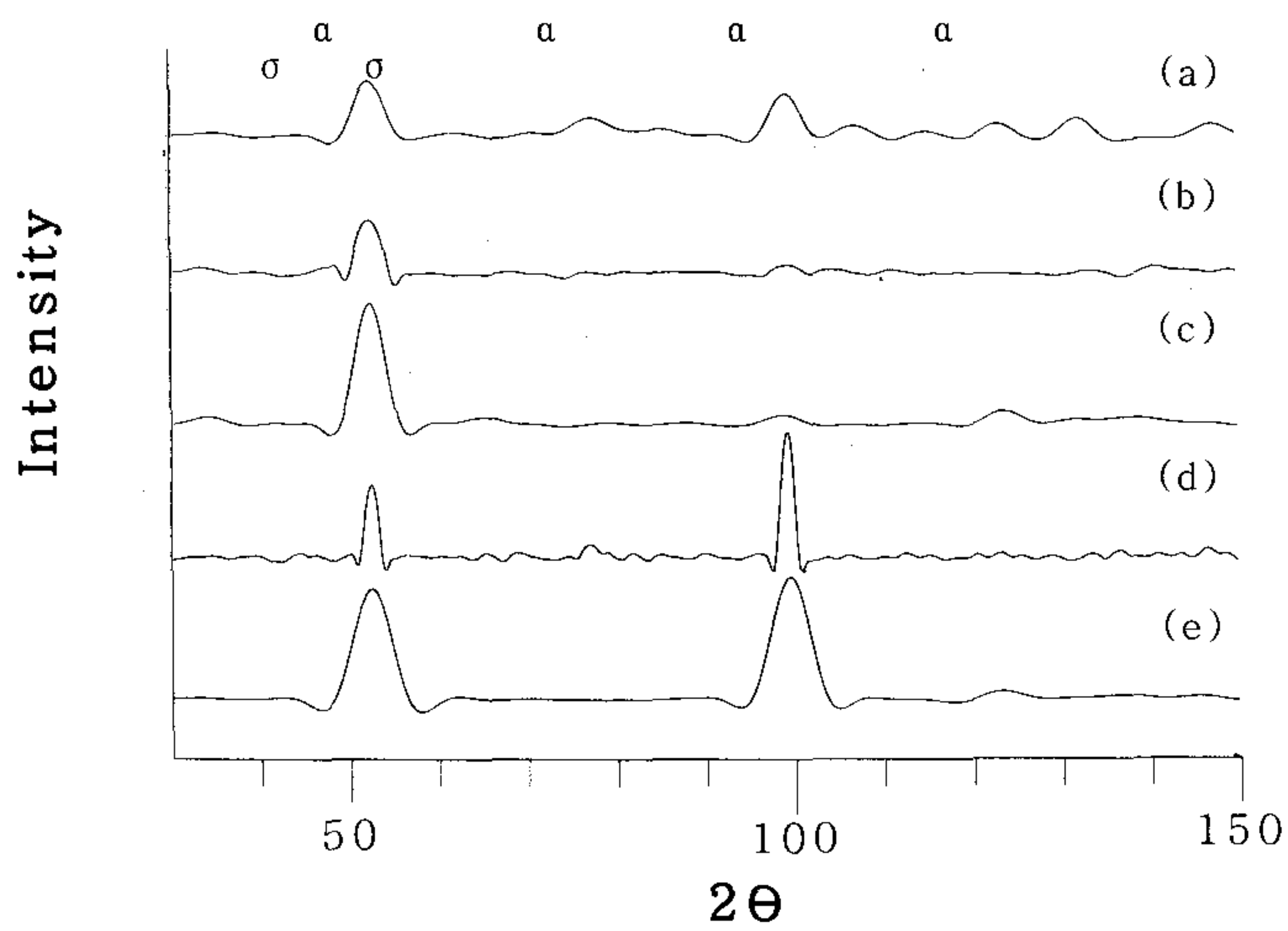

Fig. 6. The results of XRD analysis according to heat treatment conditions: (a) as- received, (b) 900 ℃ in vacuum, (c) 900 ℃ in (H_2+N_2) gas, (d) 1100 ℃ in vacuum and (e) 1100 ℃ in (H_2+N_2) gas, respectively.

hydrogen-nitrogen gas mixture (H_2 : N_2 = 1:2) or vacuum conditions. The formation of σ - phase precipitates during heat treatment was measured by XRD. The heat treatment of the materials was carried out from 600 ℃ to 1100 ℃ for 20 minutes at a heating rate of 18 ℃/min. and a cooling rate of 28 ℃/min.. Heat treatment in vacuum was also conducted at 900℃ and 1100 ℃ under a pressure of 10^{-5} Torr.

2.3 Evaluation of landing drift caused by horizontal terrestrial magnetic field

Roll-formed rails were heat-treateda at temperature ranging from 600 ℃ to 1100 ℃ and were classified into the groups according to the permeability values. Using these rails, we made products of 17″ and 19″ Flatron with modified process conditions, which will be described later. Landing drift has the largest value at the corner because the horizontal and vertical components of the electron-beam velocity are the largest and landing drift is caused by Lorentz force. In the case of a color CRT with stripe-type phosphors, discoloration does not take place when the electron beam shifts in the y-direction [9-10]. Therefore, in this study, the landing drift was measured only in the x-direction at screen corners with changes of horizontal magnetic field. Horizontal magnetic field (B_h) was set at 0 and 0.3 Gauss with a constant vertical magnetic field (B_v=0.4 Gauss). The difference between two different landing shift measurements was obtained depending on permeability, which was determined by heat treatment temperatures.

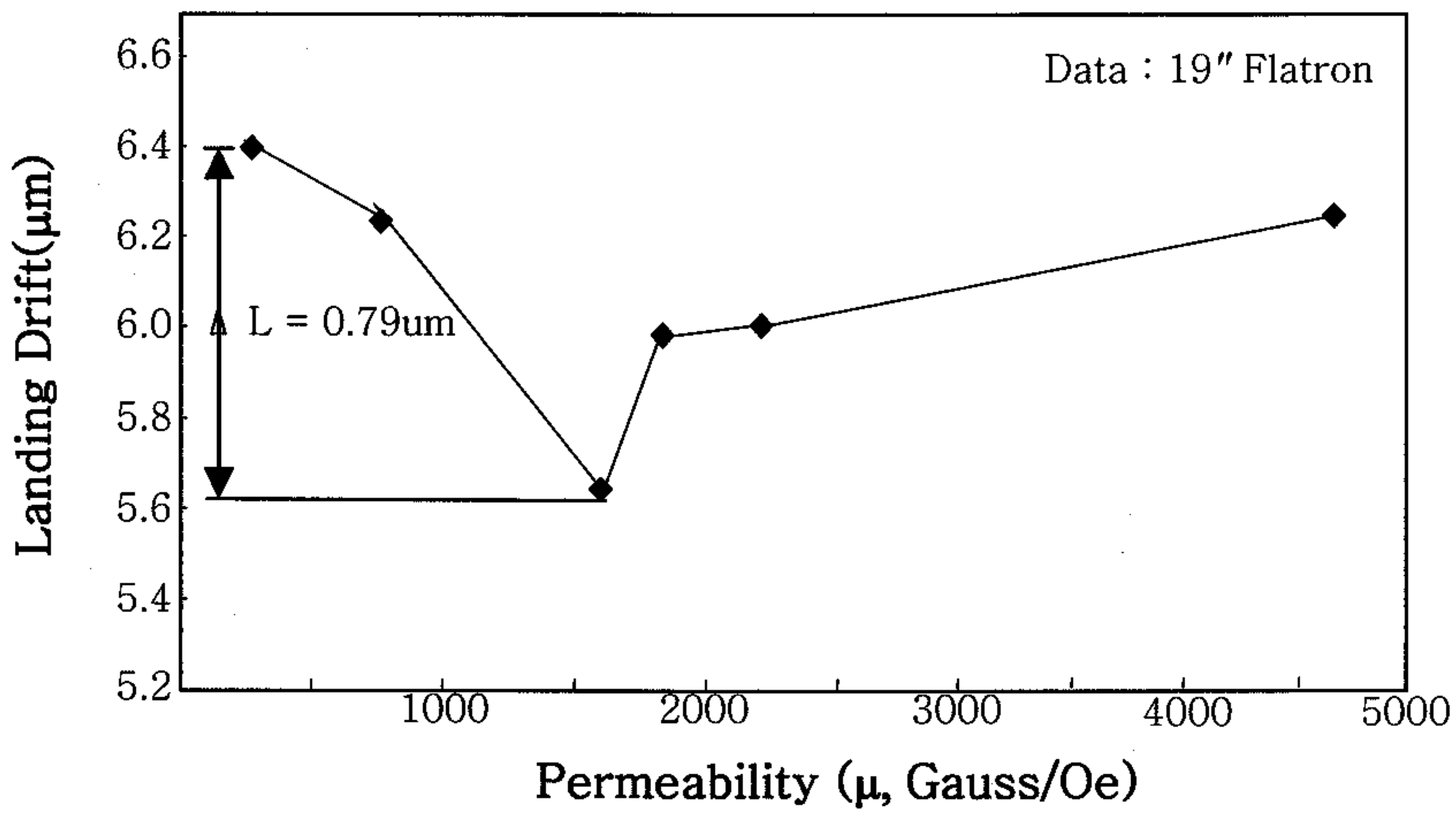

Fig. 7. Relation between permeability and landing drift measured from 19″ Flatron using the POS430Ti rail.

2.4 Experimental to diminish glass cracking

The general mechanism of crack formation is based on the difference in the coefficients of thermal expansion between the glass panel and rail. The residual stress induced during the thermal process causes glass to crack if the stress is larger than the fracture strength of glass. Equations (1) and (2) show an approximate relationship among stress, coefficient of thermal expansion and temperature.

Experimental factors should be controlled to minimize the residual stress. The controllable factors of the residual stress are the thickness of materials (M.T), end cap materials, frit-sealing temperature (F.T) and the shape of frit glass(F.S) at the corner. As shown in Table 3, $L8(2^7)$ of the orthogonal array table was adopted for the experiments [6-8]. The origin, number, and length of cracks were examined. The length of crack was adopted for a responding variable.

$$S = E \times (\alpha_p - \alpha_r) \times \Delta T \quad \cdots\cdots (1)$$

$$\alpha = \Delta L / Lo \times \Delta T \quad \cdots\cdots (2)$$

S : Stress of glass
E : Young's modulus
α_p : Thermal expansion coefficient of panel
α_r : Thermal expansion coefficient of rail
L : Length of specimen
ΔT : Difference in temperature

After analysis-of-variances (ANOVA) was carried out for the measured data of the cracks, the significant/non-significant factors were selected by P-value. We also analyzed the-smaller-the-better in Signal to Noise (S/N) ratio as shown in Equation (3), which is the index of evaluation of stability in the Taguchi method [7-8]. From the overall results from ANOVA and S/N ratio, the conditions for non-cracking were optimized.

$$\eta = -10\log \sigma^2 = -10\log \{(\Sigma yi^2)/n\} \quad \cdots\cdots (3)$$

η : S/N ratio
σ : Standard deviation
yi : Measured data
n : Number of data

3. Results and Discussion

3.1 Permeability characteristic as a function of heat treatment temperature

Fig. 3 shows that permeability values of POS430Ti and 28 wt%Cr alloy increase with the rise in temperature up to 900 ℃ and then decrease at 1100 ℃, while permeability of POS446M increases up to 1100 ℃ without any sign of decrement. This phenomenon can be explained by the following four reasons : i) change in grain size in accordance with heat treatment temperature; ii) the thickness of the oxidation layer; iii) the formation of σ - phase during heat treatment; and iv) the effects of minor elements in the alloy. Fig. 4 shows the grain growth of POS446M with increased temperature, resulting in an increase in magnetic flux. However, permeability values of POS430Ti and 28 wt% Cr alloy

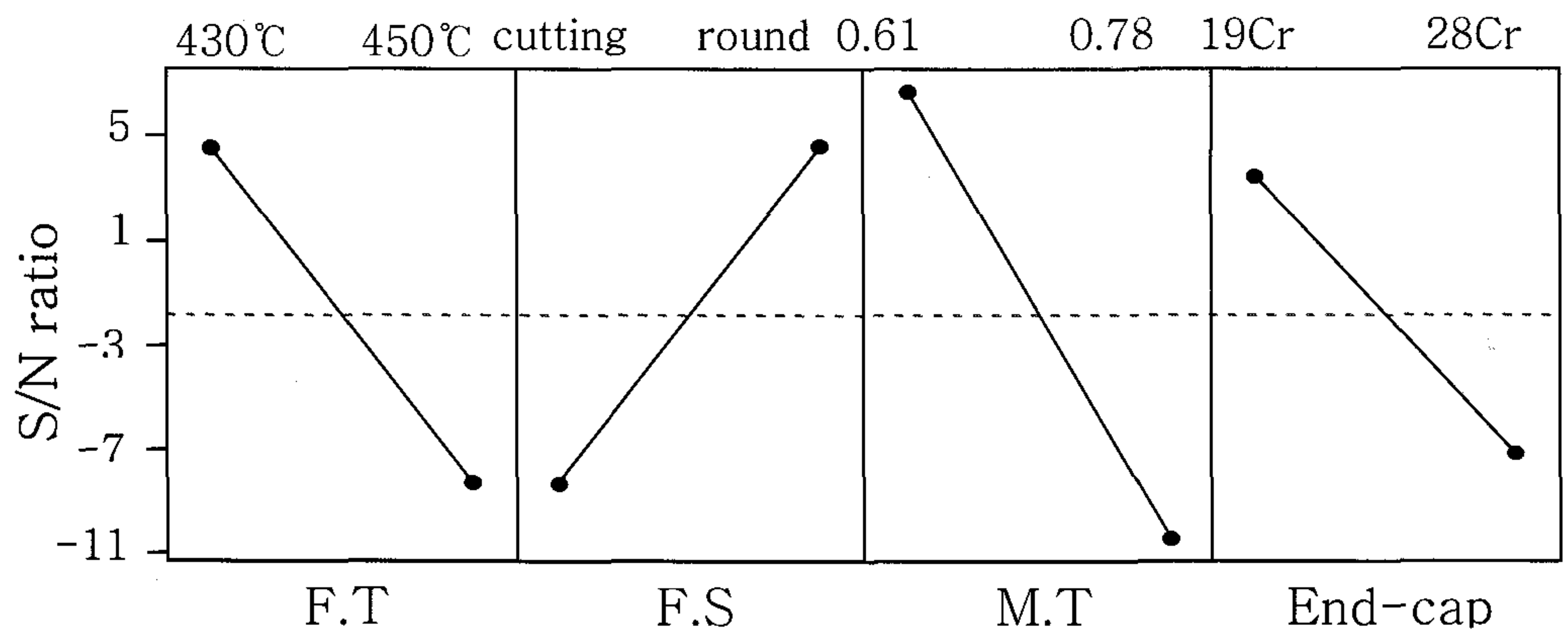

Fig. 8. Signal to Noise (S/N) ratio depending upon levels of factors.

after at 1100℃ decreased even though their grain sizes were bigger than those at 900℃. The occurrence of this phenomenon could be the result of the following two factors. First, the variation of thickness in oxidation layer induced lower magnetic flux and lower permeability. Second, σ - phase may have formed during heat treatment that caused the permeability to be reduced.

Actually, when high Cr alloy is heat treated, σ - phase is easily forms. To prove whether our assumption is correct, the specimens were heat-treated at 900 ℃ and 1100 ℃ in vacuum; measured permeability values are presented in Fig 3. As seen in the figure, the permeability values of POS430Ti and 28 wt% Cr alloy had increased again. Furthermore, in the case of POS430Ti, the thickness of the oxidation layer heat-treated at 1100 ℃ was almost three times thicker than that at 900 ℃, as seen in Fig. 5. On the other hand, Fig. 6 shows the XRD analysis of POS446M as a function of temperature and environment. It has been found that σ - phase peak does not appear even after heat treatment at 1100 ℃ and only α - phase exists. Therefore, it could be suggested that the Mo element in POS446M plays a role in enhancing anti-oxidation characteristics, and that may be the reason why the permeability of POS446M does not decrease even at high temperatures.

3.2 The amount of landing drift caused by horizontal terrestrial magnetic field

Fig. 7 shows the relationship between the landing drift and permeability. While the permeability changes from 723 to 4850 (Gauss/Oe), maximum landing drift was very small (0.8 μm). This means that landing drift is not overly affected by the permeability of materials. Actually, it has been reported that the terrestrial magnetic field in CRT affected by various parts such as the inner magnetic shield, mask, frame, band, etc [9-10]. In the case of a 19″ Flatron, however, the rail does not induce the magnetic field as much as in the CRT because the height ratio of the rail to shield in the axial direction is very small (0.031 μm).

3.3 Flatron fabrication process for prevention of cracking

As shown in Table 4, the results of ANOVA suggest that significant factors (i.e. having a 90 % confidence level) are the thickness of materials (marked M.T in Table 4) having a P-value of 0.000 and the shape of frit glass (marked F.S in Table 4) at the corner having a P-value of 0.098. Non-significant factors are the kind of end-cap and the temperature of frit sealing (marked F.T in Table 4). Although these P values do not satisfy the statistical significant level, they are assumed from a technical viewpoint to affect the formation of cracks. This is also confirmed by the Signal to Noise (S/N) ratio, as shown in Fig. 8. From the examination of the S/N ratio, the optimum rail thickness for applying POS430Ti to the Flatron rail is 0.61 mm, which is more advantageous in terms of cost saving. In addition, a round-type frit glass is better for non-cracking than a cutting-type. As far as materials for end-caps are concerned, POS430Ti is more desirable, which is the same material as the rail body. It is also found that the proper frit sealing temperature is 430 ℃ rather than 450 ℃ in preventing cracking. As a result, a Flatron rail manufacturing process using POS430Ti was stabilized without glass cracking by the application of above conditions.

4. Conclusion

In the present study, POS446M and POS430Ti alloys were investigated to be applied to the Flatron rail in place of conventional 28 wt%Cr alloy to reduce the cost of materials. It was found that the perm abilities of POS430Ti and 28 wt%Cr alloy increased up to a heat treatment temperature of 900 ℃ under a H_2+N_2 atmosphere and then decreased at 1100 ℃ due to increments in thickness of the oxidation layer on the surface. However, the permeability of POS446M did not decrease even when the heat treatment temperature increased up to 1100 ℃. The landing drift of Flatron was not affected by the change in the permeability values between the range of 700 and 5000 Gauss/Oe. In the case of POS430Ti, the significant factor causing glass cracking was the thickness of material. As a result, a Flatron rail manufacturing process using POS430Ti was stabilized without glass cracking by the application of the modified process conditions, which were optimized through the design of the experiment method.

References

[1] IDC. *DC Japan Multiclient Study LCD Quarterly Survey Fourth*, 39 (1999).

[2] Nikkei Microdevices, *Flat Panel Display 1999* (1999).

[3] Ross Young, *PD Market and Technology Trends and Forecast*, www.displaysearch.com (2000).

[4] Soo-Ho Park, Yun-Yong Lee, Yong-Deuk Lee, and Hak Kim, *Journal of the Korean Inst. of Met. & Mater.*, **36**, 78 (1998).

[5] Soo-Ho Park, Yun-Yong Lee, Yong-Deuk Lee, and Hak Kim, *Journal of the Korean Inst. of Met. & Mater.*, **34**, 1061 (1998).

[6] G.E.P. Box, W.G. Hunter and J.S. Hunter, *Statistics for Experimenters*, (John Wiley & Sons Inc., 1978), p. 235.

[7] Genichi Taguchi, Yu-In Wu, *Introduction to Off-Line Quality Control* (Central Japan Quality Control Association, 1979).

[8] Genichi Taguchi, *Introduction to Quality Engineering*, (Asian Productivity Organization, 1986), ch. 2.

[9] Ichiroh Saitoh, Siroh Kenmotsu, Tomio Aoki, and Kunikazu Tomita, *The transactions of the institute of electronics, information and communication engineers*, **J81-C**, 818-825 (1998).

[10] Akira Haga, Hiroshi Nasuno and Hideo Ikeda, in *Proceedings of the Sixth IDW*(1999), p. 485.